η-meson production in nucleon-nucleon collisions within an effective Lagrangian model

R. Shyam
Saha Institute of Nuclear Physics, Kolkata 70064, India
(Received 22 December 2006; published 8 May 2007)

We investigate the $pp \to pp\eta$ and $pn \to pn\eta$ reactions within an effective Lagrangian model for laboratory kinetic energies ranging from very close to the η-meson production threshold to about 10 GeV. Production amplitudes include contributions from the mechanisms of excitation, propagation, and decay of $N^*(1535)$, $N^*(1650)$, and $N^*(1710)$ baryonic resonances. The initial interaction between two incoming nucleons is modeled by the exchange of π, ρ, ω, and σ mesons where the vertex parameters are taken to be the same as those used in the previous applications of this model. Parameters of the resonance vertices also are taken from our earlier studies wherever applicable. Calculations are done for total as well as differential η-production cross sections. To describe the data for energies closer to the production threshold, final state interactions among the outgoing particles are included by means of a generalized Watson-Migdal method. Terms corresponding to the excitation of $N^*(1535)$ resonance and the pion exchange process dominate the cross sections. With a single set of vertex parameters, our model describes well the available data on total cross sections for beam energies ranging from close to threshold to up to 10 GeV.

DOI: 10.1103/PhysRevC.75.055201 PACS number(s): 13.60.Le, 13.75.Cs, 11.80.−m, 12.40.Vv

I. INTRODUCTION

The low energy behavior of the quantum chromodynamics (QCD) is not accessible to the perturbative approaches; the lattice gauge theory [1] is the ideal tool for this purpose. Despite the enormous computational power necessary for the numerical realization, lattice QCD calculations have started, very recently, to describe masses and other constants of the baryonic ground as well as excited states [2]. Experimentally, the determination of baryonic resonance properties proceeds indirectly by exciting the nucleon with the help of a hadronic or electromagnetic probe and performing measurements for their decay products (mesons and nucleons). The reliable extraction of nucleon resonance properties from such experiments is a major issue of the hadron physics.

In recent years, important advances have been made in the experimental investigation of meson production reactions in nucleon-nucleon (NN) collisions, particularly at beam energies very close to the respective production thresholds [3–15]. Low incident energies also provide the opportunity to investigate the meson-nucleon interactions through these reactions, since in this energy regime the final state interactions among the outgoing particles affect strongly the meson production cross sections.

The η meson, which is the next lightest nonstrange member in the meson mass spectrum, has been a subject of considerable interest. It has been thought of as a probe for the $s\bar{s}$ component in the nucleon wave function [16]. There is also interest in measuring the rare decays of η which could provide a new rigorous test of the standard model [17] or even of the physics beyond this. The nucleon resonance $N^*(1535)$ [$S_{11}(1535)$] with spin $\frac{1}{2}$, isospin $\frac{1}{2}$, and odd parity, has a remarkably large ηN branching ratio. It lies very close to the threshold of the $NN \to NN\eta$ reaction and contributes to the amplitude of this reaction even at the threshold. Therefore, the study of η-meson production in NN collisions at the near threshold beam energies provides the unique opportunity to investigate the properties of $N^*(1535)$, which have been the subject of some debate recently (see, e.g., Ref. [18]). The attractive nature of the η-nucleon interaction may lead to the formation of bound (quasibound) η-nucleus states (see, e.g., Refs. [19–23]). This subject has been a topic of intense discussion at a recent work shop [24].

Production of η meson in heavy ion collisions also is of great interest. Because of the high threshold of the elementary production reaction, η mesons in such collisions are produced only by very energetic nucleons and reflect, therefore, the tails of the nucleon momentum distributions as they arise in a high density and high temperature phase of the collision [25]. The elementary $NN\eta$ production cross sections are a crucial ingredient in the transport model studies of η-meson production in nucleus-nucleus collisions.

Since lattice QCD calculations are still far from being amenable to the low and intermediate energy scattering and reaction processes, the effective methods are mostly used for the description of the dynamics of the meson production reactions in hadronic collisions. These approaches introduce the baryonic resonance states explicitly in their framework and try to extract their properties by comparing the theoretical results with experimental observables. Several authors have used models of such type in describing the η-meson production in NN collisions [26–32].

The main objective of this paper is to investigate η-meson production in NN collisions in the framework of an effective Lagrangian model (ELM) which has been used rather successfully to describe the pion [33,34], associate kaon [35], and dilepton [36] production data in such collisions. The motivation here is to see how far one can explain the recently measured data on total and differential cross sections of $pp \to pp\eta$ [11–15] and the $pn \to pn\eta$ [10] reactions within this model using the same set of entrance channel and resonance channel parameters that was used in the model's previous applications [35,36].

Within the ELM, the initial interaction between two incoming nucleons is modeled by an effective Lagrangian which is based on the exchange of π, ρ, ω, and σ mesons. The coupling constants at the nucleon-nucleon-meson vertices are determined by directly fitting the T matrices of the NN scattering in the relevant energy region [37]. The effective Lagrangian uses the pseudovector (PV) coupling for the nucleon-nucleon-pion vertex, because it is consistent with the chiral symmetry requirement of the QCD [38–40] and because it leads to negligible contributions from the negative energy states (pair suppression phenomena) [41]. The η-meson production proceeds via excitation of $N^*(1535)$, $N^*(1650)$, and $N^*(1710)$ intermediate baryonic resonance states which have known branching ratios for the decay into the ηN channel. The coupling constants at the resonance-nucleon-meson vertices are determined from the experimental widths for the decay of the resonances into the relevant channels except for those involving the ω meson, for which they are determined from the vector meson dominance (VMD) hypothesis. The interference terms between amplitudes corresponding to various meson exchanges and the intermediate resonance states have been included.

The final state interaction (FSI) among the outgoing particles strongly affects the cross sections of the $NN \to NN\eta$ reaction at near threshold beam energies [29,30,32]. In applications of the ELM to describe the near threshold meson production reactions in NN collisions [34,35], the FSI effects were included within the Watson-Midgal theory [42] which is based on the assumption that the FSI effects are strong in relation to the production process and that they occur attractively between only one particular pair of outgoing particles. In Ref. [35], this method was used somewhat arbitrarily for all three outgoing pairs of particles. However, Watson's method as such is not applicable, in a strict sense, to those cases in which the attraction between outgoing particles is not so pronounced or where the interaction between more than one pair is to be included in the calculations. In this paper, we employ a generalized Watson method in which three-body states are treated by splitting the total interaction into pairwise net interactions which leads to a series decomposition of the net scattering among all the particles in terms of separate total scattering between pairs of particles (see, e.g., Ref. [43]). However, the three-body interactions are neglected. In view of the arguments presented in Refs. [32,44] in favor of using the three-body scattering theory to describe the $NN\eta$ process, it would be interesting to see to what extent this generalized method is able to explain the $NN\eta$ production data.

In the next section, a brief description of the ELM covers the main ingredients of the theory and gives all the input parameters used in our calculations. The generalized Watson method of FSI effects is also described. The results of our calculations are presented and discussed in Sec. III. Summary and conclusions of our work are given in Sec. IV.

II. FORMALISM

A representative of the lowest order Feynman diagrams contributing to the η-meson production considered by us is shown in Fig. 1. Momenta of various particles are indicated in Fig. 1(a). q, p_i, and p_η are four-momenta of the exchanged meson, the intermediate resonance, and the η-meson, respectively. To evaluate various amplitudes, we used the effective Lagrangians for the nucleon-nucleon-meson and resonance-nucleon-meson vertices as described below.

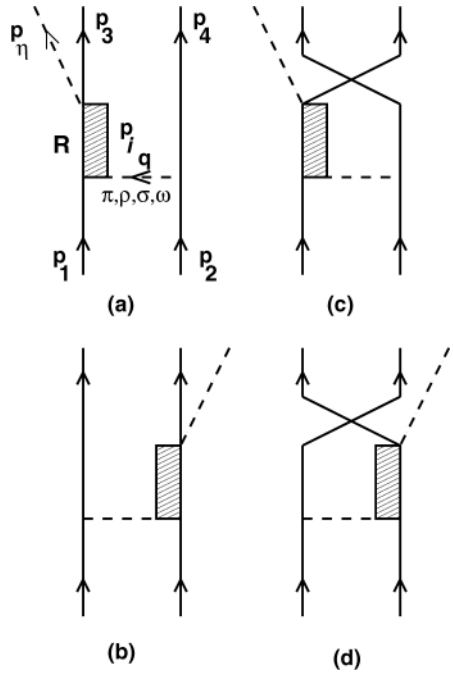

FIG. 1. Feynman diagrams for η-meson production in nucleon-nucleon collisions. Diagrams (a) and (b) show direct processes; (c) and (d) exchange ones. R represents a baryonic resonance.

A. Nucleon-nucleon-meson vertex

As done before in the investigation of $pp \to pp\pi^0$, $pp \to pn\pi^+$ [33], $pp \to p\Lambda K^+$ [35], and $NN \to NNe^+e^-$ [36] reactions, the parameters for nucleon-nucleon-meson vertices are determined by fitting the NN elastic scattering T matrix with an effective NN interaction based on the π, ρ, ω, and σ meson exchanges. The effective NN-meson Lagrangians are (see, e.g., Refs. [45,46])

$$\mathcal{L}_{NN\pi} = -\frac{g_{NN\pi}}{2m_N}\bar{\Psi}_N\gamma_5\gamma_\mu\boldsymbol{\tau}\cdot(\partial^\mu\boldsymbol{\Phi}_\pi)\Psi_N, \quad (1)$$

$$\mathcal{L}_{NN\rho} = -g_{NN\rho}\bar{\Psi}_N\left(\gamma_\mu + \frac{k_\rho}{2m_N}\sigma_{\mu\nu}\partial^\nu\right)\boldsymbol{\tau}\cdot\boldsymbol{\rho}^\mu\Psi_N, \quad (2)$$

$$\mathcal{L}_{NN\omega} = -g_{NN\omega}\bar{\Psi}_N\left(\gamma_\mu + \frac{k_\omega}{2m_N}\sigma_{\mu\nu}\partial^\nu\right)\omega^\mu\Psi_N, \quad (3)$$

$$\mathcal{L}_{NN\sigma} = g_{NN\sigma}\bar{\Psi}_N\sigma\Psi_N. \quad (4)$$

In Eqs. (1)–(4), we used the notation and conventions of Bjorken and Drell [47], and the definitions of various terms are the same as those given there. In Eq. (1), m_N denotes the nucleon mass. Note that we use a PV coupling for the $NN\pi$ vertex. Since these Lagrangians are used to directly model the NN T matrix, we also included a nucleon-nucleon-axial-vector-isovector vertex, with the effective Lagrangian

given by

$$\mathcal{L}_{NNA} = g_{NNA}\bar{\Psi}\gamma_5\gamma_\mu\boldsymbol{\tau}\Psi\cdot\mathbf{A}^\mu, \tag{5}$$

where **A** represents the axial-vector meson field. This term is introduced because if the mass of the axial meson A is chosen to be very large ($\gg m_N$) [37] and g_{NNA} is defined as

$$g_{NNA} = \frac{1}{\sqrt{3}} m_A \left(\frac{g_{NN\pi}}{2m_N}\right), \tag{6}$$

it cures the unphysical behavior in the angular distribution of NN scattering caused by the contact term in the one-pion exchange amplitude. It should be mentioned here that A is different from the $a_1(1260)$ meson resonance. The role of the A vertex is to explicitly subtract out the contact term of the one-pion exchange part of the NN interaction. A similar term in the coordinate space potential is effectively switched off by the repulsive hard core.

At each interaction vertex, the following form factor is introduced

$$F_i^{NN} = \left(\frac{\lambda_i^2 - m_i^2}{\lambda_i^2 - q_i^2}\right), \quad i = \pi, \rho, \sigma, \omega, \tag{7}$$

where q_i and m_i are the four-momentum and mass of the ith exchanged meson, and λ_i is the corresponding cutoff parameter. The latter governs the range of suppression of the contributions of high momenta which is done via the form factor. Since NN scattering cross sections decrease gradually with the beam energy (beyond a certain value), and since we fit the elastic T matrix directly, the coupling constants are expected to be energy dependent. Therefore, while keeping the cutoffs λ_i [in Eq. (7)] energy independent, we take energy-dependent meson-nucleon coupling constants of the form

$$g(\sqrt{s}) = g_0 \exp(-\ell\sqrt{s}), \tag{8}$$

where s is the square of the total c.m. energy. The parameters g_0, ℓ, and λ were determined by fitting to the T matrices of the relevant proton-proton and proton-neutron scattering data at beam energies in the range of 800 MeV to 4.00 GeV [37]. This procedure also fixes the signs of the effective Lagrangians [Eqs. (1)–(5)]. The values of various parameters are shown in Table I (the signs of all the coupling constants g are positive). In this table, the parameters of the A exchange vertex are not explicitly shown, as they are related to those of the pion via Eq. (6). We would like to remark that the same parameters were also used to describe the initial NN interaction in the calculations reported in Refs. [33,35,36]. This ensures that the elastic NN elastic scattering channel remains the same in the description of various inelastic processes within this model.

The main criterion for choosing the meson exchanges as discussed above is to describe the NN scattering in the relevant beam energy region. We have left out the η-meson exchange in our description of the NN interaction, because the contribution of the exchange terms of this particle (having a mass much larger than that of the pseudoscalar pion) is expected to be very small on account of the pseudoscalar (PS) nature of its coupling. Furthermore, the coupling constant for the $NN\eta$ vertex is small, as confirmed by several studies (see, e.g., Refs. [48–51]).

TABLE I. Coupling constants for NN-meson vertices used in calculations.

Meson	$g^2/4\pi$	ℓ	Λ (GeV)	Mass (GeV)
π	12.562	0.1133	1.005	0.138
σ	2.340	0.1070	1.952	0.550
ω	46.035	0.0985	0.984	0.783
ρ	0.317	0.1800	1.607	0.770
$k_\rho = 6.033$, $k_\omega = 0.0$				

B. Resonance-nucleon-meson vertex

As the η meson has zero isospin, only isospin-$\frac{1}{2}$ nucleon resonances are allowed. Below 2 GeV c.m. energy, $N^*(1535)$ has a prominent decay branching ratio of 40–60% into the $N\eta$ channel (see, e.g., the latest review of the Particle Data Group [52]). On the other hand, $N^*(1650)$ and $N^*(1710)$ resonances have small but non-negligible decay branching ratios of 3–10% and 6 ± 1%, respectively, to this channel. Compared to these, the branching ratio for the decay of $N^*(1520)$ resonance to $N\eta$ channel is negligibly small, and we have not included it in our description. In several previous studies of the $NN \to NN\eta$ reaction, contributions from only the $N^*(1535)$ resonance have been considered.

Since all three resonances can couple to the meson-nucleon channels considered in the previous section, we require the effective Lagrangians for all four resonance-nucleon-meson vertices corresponding to all the included resonances. At the spin-$\frac{1}{2}$ resonance $N - \pi$ (η) vertices, we have the choice of PS or PV couplings. The corresponding effective Lagrangians can be written as [35,48,53,54]

$$\mathcal{L}^{PV}_{N^*_{1/2}N\pi} = -\frac{g_{N^*_{1/2}N\pi}}{M}\bar{\Psi}_{N^*}\Gamma_\mu\boldsymbol{\tau}\cdot(\partial^\mu\boldsymbol{\Phi}_\pi)\Psi_N + \text{h.c.}, \tag{9}$$

$$\mathcal{L}^{PS}_{N^*_{1/2}N\pi} = -g_{N^*_{1/2}N\pi}\bar{\Psi}_{N^*} i\Gamma\boldsymbol{\tau}\boldsymbol{\Phi}_\pi\Psi_N + \text{h.c.}, \tag{10}$$

$$\mathcal{L}^{PV}_{N^*_{1/2}N\eta} = -\frac{g_{N^*_{1/2}\eta}}{M}\bar{\Psi}_{N^*}\Gamma_\mu\boldsymbol{\tau}\cdot(\partial^\mu\boldsymbol{\Phi}_\eta)\Psi_N + \text{h.c.}, \tag{11}$$

$$\mathcal{L}^{PS}_{N^*_{1/2}N\eta} = -g_{N^*_{1/2}N\eta}\bar{\Psi}_{N^*} i\Gamma\boldsymbol{\tau}\boldsymbol{\Phi}_\eta\Psi_N + \text{h.c.}, \tag{12}$$

where $M = (m_{N^*} \pm m_N)$, with the upper sign for even parity and lower sign for odd parity resonance. The operators Γ, Γ_μ, are given by

$$\Gamma = \gamma_5, \quad \Gamma_\mu = \gamma_5\gamma_\mu, \tag{13}$$

$$\Gamma = 1, \quad \Gamma_\mu = \gamma_\mu, \tag{14}$$

for resonances of even and odd parities, respectively. We performed calculations with both of these couplings. The effective Lagrangians for the coupling of resonances to other mesons are

$$\mathcal{L}_{N^*_{1/2}N\rho} = -g_{N^*_{1/2}N\rho}\bar{\Psi}_{N^*}\frac{1}{2m_N}\Gamma_{\mu\nu}\partial^\nu\boldsymbol{\tau}\cdot\boldsymbol{\rho}^\mu\Psi_N + \text{h.c.}, \tag{15}$$

$$\mathcal{L}_{N^*_{1/2}N\omega} = -g_{N^*_{1/2}N\omega}\bar{\Psi}_{N^*}\frac{1}{2m_N}\Gamma_{\mu\nu}\partial^\nu\omega^\mu\Psi_N + \text{h.c.}, \tag{16}$$

$$\mathcal{L}_{N^*_{1/2}N\sigma} = g_{N^*_{1/2}N\sigma}\bar{\Psi}_{N^*}\Gamma'\sigma\Psi_N + \text{h.c.}, \tag{17}$$

where operators Γ' and $\Gamma_{\mu\nu}$ are

$$\Gamma' = 1, \quad \Gamma_{\mu\nu} = \sigma_{\mu\nu} \tag{18}$$

$$\Gamma' = \gamma_5, \quad \Gamma_{\mu\nu} = \gamma_5\sigma_{\mu\nu}, \tag{19}$$

for resonances of even and odd parities, respectively.

We assume that the off-shell dependence of the NN^* vertices are determined solely by multiplying the vertex constants by form factors. Similar to Refs. [46,55], we use the following form factors for N^*N-meson vertices:

$$F_i^{NN^*} = \left[\frac{\left(\lambda_i^{N^*}\right)^4}{\left(\lambda_i^{N^*}\right)^4 + \left(q_i^2 - m_i^2\right)^2}\right], \quad i = \pi, \rho, \sigma, \omega. \tag{20}$$

The resonance couplings are determined from the experimentally observed branching ratios for the decay of the resonances to the corresponding channels. Since the resonances considered in this study have no known branching ratios for the decay into the $N\omega$ channel, we determine the coupling constants for the $N^*N\omega$ vertices by the strict vector meson dominance (VMD) hypothesis [56], which is based essentially on the assumption that the coupling of photons to hadrons takes place through a vector meson. For details of these calculations, refer to Ref. [35].

The resonance properties and values of various coupling constants are given in Table II. Value of the cutoff parameter ($\lambda_i^{N^*}$) is taken to be 1.2 GeV for all the vertices, which is the same as that used in Refs. [36,55]. Fixing $\lambda_i^{N^*}$ to one value minimizes the number of free parameters.

It should, however, be stressed that the branching ratios determine only the square of the corresponding coupling constants, thus their signs remain uncertain in this method. Predictions from independent studies are used as a guide to fix these signs. We followed here the results of Ref. [46] for this purpose. The propagators for various meson and nucleon resonances in the calculation of the amplitudes were taken to be the same as those discussed in Refs. [35,36].

TABLE II. Resonance parameters and coupling constants for various decay vertices. Coupling constants at $N^*N\omega$ vertices are obtained from the vector-meson dominance hypothesis (see, e.g., Ref. [35]).

Resonance	Width (GeV)	Decay channel	g
$N^*(1535)$	0.150	$N\pi$	0.6840
		$N\rho$	3.9497
		$N\omega$	1.4542
		$N\sigma$	2.5032
		$N\eta$	2.2000
$N^*(1650)$	0.150	$N\pi$	0.8096
		$N\rho$	2.6163
		$N\omega$	1.8013
		$N\sigma$	2.5032
		$N\eta$	−0.5469
$N^*(1710)$	0.150	$N\pi$	1.0414
		$N\rho$	2.9343
		$N\omega$	1.5613
		$N\sigma$	0.6737
		$N\eta$	1.0328

TABLE III. Isospin factors for various diagrams. Isovector corresponds to π and ρ exchange graphs; isoscalar, to ω and σ ones.

Graph	Isovector	Isoscalar
	$pp \to pp\eta$	
Direct	1.0	1.0
Exchange	1.0	1.0
	$pn \to pn\eta$	
Direct	−1	1
Exchange	2	0

C. Amplitudes and cross sections

Having established the effective Lagrangians, coupling constants, and form of the propagators, we can calculate the amplitudes for various diagrams associated with the $NN \to NN\eta$ reaction in a straight forward manner by following the well-known Feynman rules. The isospin part is treated separately. This gives rise to a constant factor for each graph, as shown in Table III.

It should be stressed here that signs of various amplitudes are fixed by those of the effective Lagrangians, coupling constants, and propagators as described above. These signs are not allowed to change anywhere in the calculations.

The general formula for the invariant cross section of the $NN \to NN\eta$ reaction is written as

$$d\sigma = \frac{m_N^4}{2\sqrt{\left[(p_1 \cdot p_2)^2 - m_N^4\right]}} \times \frac{1}{(2\pi)^5}\delta^4(P_f - P_i)|T_{fi}|^2 \prod_{a=1}^{3}\frac{d^3p_a}{E_a}, \tag{21}$$

where T_{fi} represents the total amplitude, P_i and P_f the sum of all the momenta in the initial and final states, respectively, and p_a the momenta of the three particles in the final state. The corresponding cross sections in the laboratory or c.m. systems can be written from this equation by imposing the relevant conditions.

D. Final state interaction

For describing the data for the $NN \to NN\eta$ reaction at beam energies very close to the η production threshold, consideration of the FSI among the three outgoing particles is important. We follow here an approximate scheme in line with the Watson-Migdal theory of FSI [42]. In this approach, the energy dependence of the cross section due to FSI is separated from that of the primary production amplitude. This is based on the assumption that the reaction takes place over a small region of space, a condition fulfilled rather well in near threshold reactions involving heavy mesons. This method has been extensively applied to study the low momentum behavior of the pion [34,57,58], η-meson [59–61], associated hyperon [35,62], and ϕ-meson [63] production in NN collisions. The total amplitude is written as

$$T_{fi} = T_0(NN \to NN\eta) \cdot T_{ff}, \tag{22}$$

where $T_0(NN \to NN\eta)$ is the primary production amplitude, while T_{ff} describes the re-scattering among the final particles which goes to unity in the limit of no FSI. The factorization of the total amplitude into those of the FSI and primary production [Eq. (22)] enables one to pursue the diagrammatic approach for the latter within an effective Lagrangian model and investigate the role of various meson exchanges and resonances in describing the reaction.

Watson's original method [42] was developed for those cases where the final state interaction is strong in relation to the production process and where it is confined only to one particular pair of particles (mostly among nucleons in case of nucleon-nucleon-meson final states). On the other hand, in certain cases it may be necessary to include FSI among all three outgoing particles, since even if the meson-baryon interactions are weak, they can still be influential through interference. In Ref. [35], the T matrix T_{ff} was written (without providing any proof) as a coherent sum of the transition matrices describing the final state interaction among all three two-body subsystems of the final state nucleon-nucleon-meson system. We show here that this result can be obtained (in a slightly different form) by following the technique of multiple FSI as discussed in Ref. [43]. To that end, we first try to represent the total amplitude T_{fi} in terms of an expression similar to that given by Eq. (22) where the FSI amplitude T_{ff} is appropriately constructed.

To introduce the treatment of the FSI for the three-particle system, we assume that the three-particle final states can be represented by additive potentials of the form $U = U_{12} + U_{31} + U_{23} \equiv U_3 + U_2 + U_1$. With this assumption, the total amplitude T_{fi} can be written as a iteration series in terms of the production amplitude T_0 [defined in Eq. (22)] and the three-body final state pair interaction amplitudes $T_{ij} \equiv T_k$ (see the Appendix for details).

$$T_{fi} = T_0 + \sum_k T_k G_0 T_0 + \sum_{k\neq j} T_k G_0 T_j G_0 T_0 + \cdots, \quad (23)$$

where the FSI transition matrices T_k are as defined in the Appendix. G_0 is Green's function corresponding to the free Hamiltonian (kinetic energy). Neglecting processes depicted by the third term, this decomposition can be expressed by the diagram in Fig. 2. It is easy to show that the result of the Watson FSI theory are recovered if one retains only the amplitude T_0 and a single pair amplitude, say, T_{12}.

Any practical calculation requires evaluation of the matrix element $\langle 123|T_{12}G_0T_0|N_1N_2\rangle$, where N_1 and N_2 denote two particles of the incident channel and 1, 2, and 3 represent the outgoing channel particles. Introducing a complete set of intermediate states of particles, say, 1 and 2, we get for this channel

$$T_{fi} = \frac{1}{(2\pi)^3}\int \frac{d^3\mathbf{k}_1'}{2E_1'}\frac{d^3\mathbf{k}_2'}{2E_2'}\delta^3(\mathbf{k}_1' + \mathbf{k}_2' - \mathbf{k}_1 - \mathbf{k}_2) \times \frac{\langle \mathbf{k}_1\mathbf{k}_2|T_{12}|\mathbf{k}_1'\mathbf{k}_2'\rangle\langle \mathbf{k}_1'\mathbf{k}_2'\mathbf{k_3}|T_0|N_1N_2\rangle}{E - (E_3 + E_1' + E_2') + i\epsilon}. \quad (24)$$

Note that in this form, each particle lies on the mass shell, and three-momentum is conserved in the intermediate processes. Introducing the total and relative momenta, $\mathbf{p}' = \mathbf{k}_1' + \mathbf{k}_2'$, $2q' = \mathbf{k}_1' - \mathbf{k}_2'$, and evaluating the integral in the barycentric frame of 1 and 2, we obtain

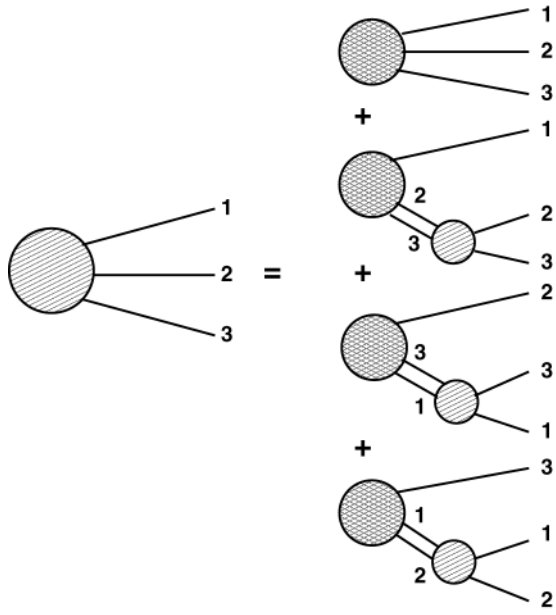

FIG. 2. Final state scattering among three particles evaluated to the lowest order.

$$T_{fi} = \frac{1}{(2\pi)^3}\int \frac{T_{12}(\xi,\theta;\xi',\theta')T_0(\xi',\theta',\mathbf{k}_3;\mathbf{k}_i)}{\xi - \xi' + i\epsilon}\frac{2q'd\xi'd\Omega'}{\xi'}, \quad (25)$$

where ξ is the energy of 1 and 2 in this frame, ξ' is the intermediate state, and θ denotes the orientation (θ, ϕ) of $\mathbf{q}$ with respect to a fixed axis.

For further evaluation of the integral, we make a partial-wave decomposition of the amplitude; for each partial wave, we rewrite the integral as

$$T_{fi}^{\ell m} \propto T_{12}(\xi,\xi)T_0(\xi) \times \int \frac{[T_{12}(\xi,\xi')T_0(\xi')/T_{12}(\xi,\xi)T_0(\xi)]}{\xi - \xi' + i\epsilon}\frac{2q'd\xi'd\Omega'}{\xi'}, \quad (26)$$

Now we make the assumption that the ratio within the square brackets in the integrand of Eq. (26) is constant up to a certain energy ξ_c and is zero thereafter. Extending this procedure to all three interacting pairs, we get in the low energy and s-wave limit,

$$T_{fi} \simeq T_0(\xi)T_{ff}(\xi). \quad (27)$$

In Eq. (27) T_{ff} is defined as

$$T_{ff}(\xi) = \sum_{i\neq j} c_{ij}T_{ij}(\xi,\xi), \quad (28)$$

where

$$c_{ij} = \frac{1}{\pi}\cosh^{-1}\left[1 + \frac{16m_i - m_j(\xi_c - m_im_j)}{(m_i + m_j)^3}\right]. \quad (29)$$

It is obvious that Eq. (28) allows interference among the final state scattering amplitudes. We further note that apart from the factor c_{ij}, this equation is similar to that used in Ref. [35].

The derivation of Eq. (27) is independent of the strength of the interaction and of whether it is attractive or repulsive. The quantity c_{ij} can be regarded as the amount of final state scattering that takes place in a particular channel ij. A plausible value of the cutoff ξ_c comes from the constraint that for the NN substate, c_{ij} should come out to be unity since in the limit of FSI in only this substate, we should recover Watson's result. With the same value of ξ_c, the c_{ij} for the ηN substate comes out to be 1.07. Note, however, that this procedure determines the value of the c_{ij} at best only for the NN channel. It remains largely undetermined for the $\eta - p$ substate, which could even be dependent on the relative energy of this channel. Since, for the time being, we do not have a definite method to determine this quantity, we have taken the same value for the parameter ξ_c for both substates.

For calculating the FSI amplitude for the ηN substate, we note that there are no direct measurements of the elastic ηN scattering and the information about the ηN elastic scattering amplitude has to be obtained by describing the $\pi N \to \eta N$ and $\gamma N \to \eta N$ data within some model. Recently, it was suggested that the ηN scattering amplitude be determined from the studies of associated photoproduction of ϕ and η mesons off the proton [64]. We adopt here the results reported in Ref. [65], where ηN scattering parameters were obtained by fitting the $\pi N \to \pi N, \pi N \to \eta N, \gamma N \to \eta N$ data in an energy range from threshold to about 100 MeV, in a K matrix method. These authors write the elastic ηN scattering T matrix as

$$T^{-1} = 1/a + \frac{r_0}{2} q_\eta^2 + s q_\eta^4 - i q_\eta, \tag{30}$$

where q_η is the momentum in the ηN c.m. system. Seven sets of values of the parameters a, r_0, and s are given in Ref. [65]. We found that the best description of the data (within the realm of our overall input parameter sets given in Tables I and II), is provided by the ηN scattering amplitudes with the parameter set $a = 0.51 + i0.26$ fm, $r_0 = -2.50 - i0.310$ fm, and $s = -0.20 - i0.04$ fm^3. Note that the real part of the ηN scattering length of this parameter set (a_R) is about half that of the preferred set of Ref. [65]. A larger a_R is also supported by the calculations presented in Ref. [66]. However, we note that in the theoretical description of the $pp \to pp\eta$ reaction as reported in Refs. [27,67], the value of a_R was similar to that used by us. A smaller a_R is also consistent with that extracted in Ref. [54] in an effective Lagrangian model analysis of the meson-nucleon scattering. Furthermore, Ref. [68] noted that within a three-body model, the shapes of the $np \to \eta d$ cross sections can be explained over a wide energy range only with a a_R around 0.42 fm. A smaller value of a_R is also consistent with the Jülich model [69].

The FSI amplitude T_{NN} was calculated by following the Jost function method using the effective range expansion (ERE) of the NN phase shifts, as discussed in Refs. [34,35,42]. For the proton-proton substate, the Coulomb modified ERE was used [70]. The effective range parameters for the NN channel were taken to be the same as those used in Ref. [34].

It should, however, be mentioned here that the use of on-shell forms to describe the FSI T matrices T_{ff} has been criticized by some authors. It has been argued in Refs. [71,72] that the absolute magnitudes of the cross sections obtained by such a procedure could be uncertain because of the of-shell effects. Even the Jost function method has been shown [73] to produce inadequate results in an study where the scattering length parameters for the $\Lambda - p$ final state were extracted from the $pp \to p\Lambda K^+$ data. In the next section, we examine the role of the off-shell effects in the NN substate in more detail.

III. RESULTS AND DISCUSSIONS

The major aim of this paper is to check the suitability of our model and the vertex parameters appearing therein to describe η production cross sections over a wide range of beam energies. We therefore applied our approach to describe the total cross sections for the $pp \to pp\eta$ reaction for beam energies ranging from near threshold to 10 GeV and for the $pn \to pn\eta$ reaction for beam energies from threshold to 1.6 GeV. These are the energy regimes in which experimental data are available for the two reactions. We also used this method to describe one set of the exclusive data, namely, the η angular distributions for the former reaction. Calculations were performed by using both the PS and PV couplings for $N^*N\pi$ and $N^*N\eta$ vertices. We note that the cross sections remain almost unchanged by switching from one type of coupling to another. In all the calculations shown below, the coupling constants and cutoff parameters for various vertices were the same as those discussed in Sec. II.

A cleaner check of the vertex parameters used in calculating the amplitude $T_0(NN \to NN\eta)$ is provided by comparing our calculations with the data for beam momenta above 3 GeV/c, since at these energies FSI effects are most likely to be unimportant. In Fig. 3, we compare our calculations and the experimental data (taken from Ref. [74]) for the total cross section of the $pp \to pp\eta$ reaction at higher beam energies. We notice that the measured cross sections are reproduced reasonably well by our calculations (solid line) in the entire range of beam momenta.

Individual contributions of various nucleon resonance intermediate states to the $pp \to pp\eta$ reaction are also shown in Fig. 3. Cross sections corresponding to $N^*(1535)$, $N^*(1650)$ and $N^*(1710)$ resonances are represented by dashed, dotted and dashed-dotted lines, respectively while their coherent sum

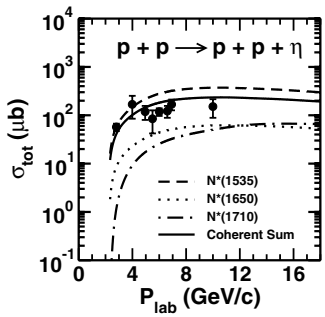

FIG. 3. Total cross section for the $p + p \to p + p + \eta$ reaction as a function of the beam momentum, showing contributions of three baryonic resonance intermediate states and their coherent sum. Experimental data are from Ref. [74].

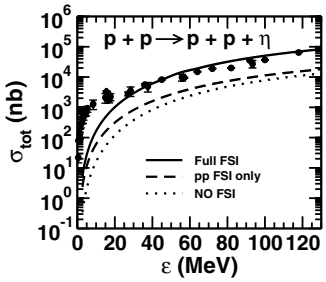

FIG. 4. Total cross sections for the $p + p \to p + p + \eta$ reaction as a function of excess energy, obtained with FSI effects included only in the pp substate of the final channel, with no FSI at all, and with full FSI effects. Experimental data are from Refs. [11–15].

is shown by the solid line. We note that the contributions of the $N^*(1535)$ resonance dominate the total cross section for all the beam momenta. In comparison, those of $N^*(1650)$ and $N^*(1710)$ resonances are smaller by factors ranging from 5 to 10. However, the interference terms of the amplitudes corresponding to various resonances are not negligible. It must again be emphasized that we have no freedom in choosing the relative signs of the interference terms.

The results shown in Fig. 3 fix the parameters of all the vertices. In the application of our model to describe $NN\eta$ data at near threshold beam energies, the amplitude $T_0(NN \to NN\eta)$ has been calculated with exactly the same values for all the parameters. For these energies, the FSI effects in the outgoing channels were included by using Eqs. (27)–(30). The experimental cross sections in this energy regime are given as a function of the excess energy ϵ, which is defined as $\epsilon = \sqrt{s} - 2m_p - m_\eta$, where $\sqrt{s}$ is the invariant mass.

In Figs. 4 and 5, we present comparisons of our calculations with the experimental data for total cross sections of the $pp \to pp\eta$ and $pn \to pn\eta$ reactions, respectively, as a function of ϵ. The lines show the results obtained by including the full FSI effects in all the three subsystems, FSI only in the pp (or pn) channel, and no FSI at all. Note that no arbitrary normalization constant has been introduced in any of the results shown in these figures. For the case of the $pp \to pp\eta$ reaction, our full calculations describe the data quite well for ϵ values in the range of 15–130 MeV. On the other hand, for the $pn \to pn\eta$ reaction, they are in excellent agreement with the available data for all the beam energies. The FSI in the ηp substate is indeed quite important in our model. The difference between results obtained with FSI in only the pp substate and that in all the three subsystems of the final channel is comparable to that reported in the three-body calculations of Ref. [32]. Those authors presented their results for ϵ values up to only 60 MeV. It would be interesting to see the results of their model also at higher values of ϵ. Note, however, that the description of the data for the $pn \to pn\eta$ reaction within the three-body model is less satisfactory than that for the $pp \to pp\eta$ reaction.

We see that the ELM can describe both the energy dependence and the absolute magnitudes of the experimental cross sections for the η-meson production in both pp and pn channels for excess energies > 15 MeV. However, it underpredicts the pp channel data for ϵ values below 15 MeV. Such a trend was also seen in calculations presented in Refs. [29,30] where the η-meson production in NN collisions was investigated within a relativistic meson exchange model including the initial state interactions and FSI only in the NN subsystem. Those authors attributed the near threshold underestimation of the experimental total cross section to the noninclusion of the ηp FSI in their model.

Since the ingredients of the primary production amplitude of our model have already been checked and fixed by calculations done at higher beam energies where FSI effects are absent, the underestimation of the $pp \to pp\eta$ cross section for very low values of ϵ indicates that we need to improve the treatment of the FSI effects. Inclusion of the off-shell effects in the calculations of FSI is one of the likely improvements. The knowledge about the off-shell nature of the ηN interaction is still very sparse. However, we can use the results presented in Ref. [61] to investigate the effects of using off-shell pp FSI on the near threshold η production cross sections. In Fig. 6, we compared the results for the total cross sections for the $pp \to pp\eta$ reaction obtained by including FSI in pp substate calculated within Jost function technique and that obtained with the method described in Ref. [61] which includes off-shell effects. In the results presented in this figure, no ηp FSI were considered. We note that the off-shell effects in the pp FSI do increase the cross section for $\epsilon < 60$ MeV. However, the increase is not enough to explain the underprediction of the experimental data by our theory at smaller energies. One needs to have a better understanding of the ηN scattering

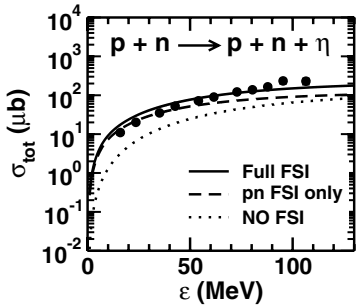

FIG. 5. Same as Fig. 4, but for the $p + n \to p + n + \eta$ reaction. Experimental data are from Ref. [10].

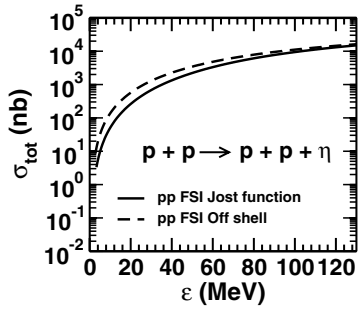

FIG. 6. Total cross section for the $p + p \to p + p + \eta$ reaction as a function of the excess energy with only the pp FSI effects calculated with the Jost function method or with the method described in Ref. [61].

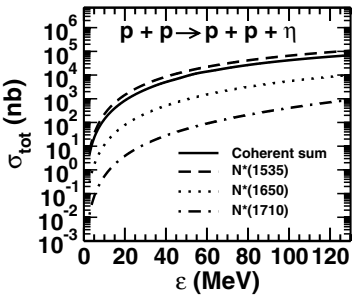

FIG. 7. Contributions of baryonic resonances to the total cross section for $pp \to pp\eta$ reaction.

amplitude. Further improvement may come by including the three-body terms in the expansion of the scattering amplitude given by Eq. (23). It has been shown in Ref. [32] that $NN\eta$ FSI effects calculated within a three-body scattering theory lead to enhanced cross sections at very low values of ϵ.

Note that the differences in the cross sections of $pn \to pn\eta$ and $pp \to pp\eta$ reactions are not only due to different isospin factors, but also due to differences in the FSI effects. The low energy scattering parameters between pp and pn are different; the latter involves also a triplet spin state together with the singlet one. A crucial difference between them is the Coulomb interaction. This is not included in the three-body model calculations of the $pp \to pp\eta$ reaction reported in Ref. [32]. Inclusion of this term is likely to reduce the cross section for beam energies very close to the threshold.

In Figs. 7 and 8, we show the individual contributions of various nucleon resonances to the total cross sections of the $pp \to pp\eta$ and $pn \to pn\eta$ reactions, respectively, at the near threshold beam energies. Similar to the situation at higher beam energies, the cross sections are dominated by the $N^*(1535)$ resonance excitation. Since $N^*(1535)$ is the lowest energy baryonic resonance having an appreciable branching ratio for the decay into the $N\eta$ channel, its dominance in this reaction even at beam energies near the η production threshold is to be expected. The contribution of the $N^*(1650)$ resonance state is small and that of the $N^*(1710)$ resonance is even smaller at these lower beam energies. Note, however, that the resonance-resonance interference terms are not negligible. For the $pp \to pp\eta$ reaction, the total cross sections are smaller than those corresponding to the $N^*(1535)$ resonance alone. For the $pn \to pn\eta$ reactions, the difference between the two is not visible in Fig. 8.

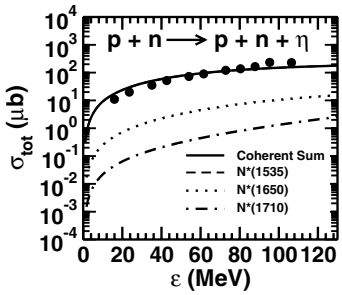

FIG. 8. Same as Fig. 7, but for the $pn \to pn\eta$ reaction.

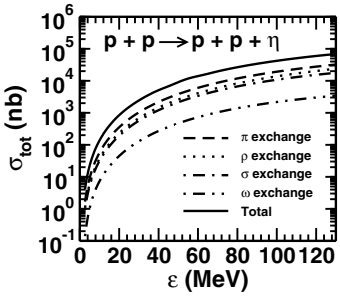

FIG. 9. Contributions of various meson exchange processes to the total cross section for the $pp \to pp\eta$ reaction as a function of the excess energy.

We found that the inclusion of the amplitudes corresponding to the nucleon intermediate states (the nucleon bremsstrahlung) made a negligible difference in the results reported in Figs. 1–8 if the value of the coupling constant $g_{NN\eta}$ was taken below 3.0. With the largest value of $g_{NN\eta}$ used in the literature (6.14), the results were affected to the extent of only a few percent. This result agrees with that reported in Ref. [29]. It is obvious that due to a considerable amount of uncertainty in the value of $g_{NN\eta}$, the nucleon excitation amplitudes are quite uncertain (see, e.g., Refs. [48,75,76]) and their inclusion makes an insignificant difference in the results reported above.

In Fig. 9, we show contributions of various meson exchanges to the $pp \to pp\eta$ reaction at near threshold beam energies. We see that the one-pion exchange graphs make the largest contribution to the reaction in this energy regime. However, a striking feature of this figure is that despite a larger value for the $g_{N^*N\rho}$ coupling used in our calculations, the contributions of ρ meson exchange are still much smaller than those of the pion exchange graphs. Hence, in contrast to the results reported in Refs. [67,77], the ρ meson exchange terms do not dominate the total $NN\eta$ production cross sections. To understand this difference, we note that while in Refs. [67,77] $\gamma_5\gamma_\mu$ couplings were used for the ρNN^* vertex, we took a $\gamma_5\sigma_{\mu\nu}$ coupling for the same which is an extension of the γNN^* couplings (due to vector-meson dominance reasons [48]). This is also compatible with the forms of the ρNN^* couplings used in the literature [46,78,79]. Since the ρ-meson exchange amplitudes calculated with the $\gamma_5\sigma_{\mu\nu}$ couplings involve delicate cancellations among leading terms, contributions of these exchange diagrams to the η production cross sections are weakened. This is the main reason for differences between our results and those of Refs. [67,77].

In Ref. [29], although the form of the ρNN^* coupling is the same as ours, relatively lower ρ meson exchange cross sections result from the use of a very small value for the coupling constant $g_{N^*N\rho}$ which is based on the lower limit of the branching ratio for the radiative decay of this resonance. Our value for this constant, on the other hand, is calculated from the branching ratio of the decay of this resonance to the $N\rho$ channel as quoted in Ref. [52].

We see that the ω-meson exchange process contributes insignificantly to the $NN\eta$ production, but the σ-meson

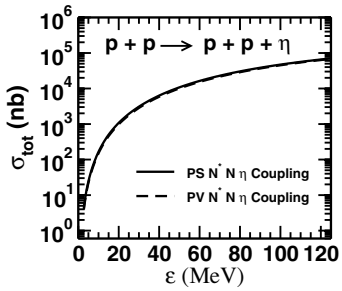

FIG. 10. Total cross section for the $pp \to pp\eta$ reaction calculated with pseudovector and pseudoscalar couplings for the $N^*N\pi(\eta)$ vertex for the resonances considered in this paper, as a function of the excess energy.

exchange terms are relatively more important. Larger contributions from the latter have also been seen in other subthreshold reactions analyzed within our model. It indicates that σ-meson exchange may be an efficient means of mediating the large momentum mismatch involve in the meson production in NN collisions [80,81].

In Fig. 10, we investigate the effects of using PS or PV couplings for the $N^*N\pi(\eta)$ vertices. We notice hardly any difference in the cross sections calculated by the two types of couplings. Similar results were also observed in Ref. [46]. This result is not surprising, since the two couplings are constructed in such a way that both are equivalent on the mass shell. Of course, they start having different energy behaviors in the far off-shell region where resonance contribution is suppressed anyway due to dominance of the corresponding propagator. It is only in the $NN\pi$ case that differences in the PS and PV couplings are obvious with a clear preference for the PV coupling in line with the chiral symmetry as discussed earlier.

After establishing the dynamical content of our model in relation to the description of the total production cross sections, we now turn our attention to more exclusive data. In Fig. 11, we compare our calculations with the data for the angular distribution of η meson in the $pp \to pp\eta$ reaction for ϵ values

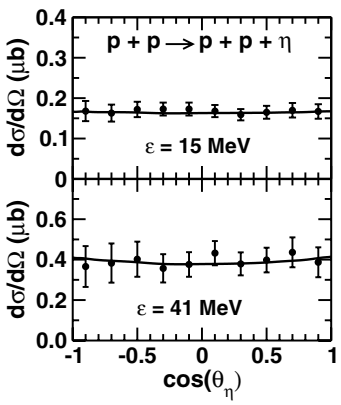

FIG. 11. Differential cross sections of the $pp \to pp\eta$ reaction as a function of η-meson angle in the c.m. frame of the total system at e excess energies of 15 and 41 MeV. Experimental data are from Ref. [8].

of 15 and 41 MeV. Since the angular distribution data are normalized to the total cross sections for both values of ϵ, we did the same in our calculations shown in this figure. We note that shapes of the angular distributions are described well by our model at both energies. At the lower beam energy, the data as well as our calculations have essentially isotropic distributions. However, for $\epsilon = 41$ MeV, our calculations tend to show slight enhancements at forward and backward angles, which is typical of the π exchange dominance process in the $N^*(1535)$ excitation. Because of large statistical errors in the data, it is difficult to conclude that they show a trend different from our calculations. It would be useful to have better quality data with less statistical errors to determine whether other mechanisms that may show a trend different from ours are also important. In any case, it is quite unlikely that the ρ-meson exchange mechanism which might lead to a distribution different from that seen in our calculations [28] is a dominant mechanism as has already been discussed.

IV. SUMMARY AND CONCLUSIONS

In this paper, we investigated the η-meson production in proton-proton and proton-neutron collisions for beam energies ranging from near threshold to about 10 GeV within an effective Lagrangian model which had been used previously to describe successfully pion, associated kaon, and dilepton production in NN collisions. The interaction between two nucleons in the initial state was modeled by the effective Lagrangians based on the exchange of π, ρ, ω, and σ mesons. The parameters of the corresponding vertices were taken to be the same as those used in the previous applications of this model, which restricts the freedom of varying the parameters to get fits to the data. The η-meson production proceeds via excitation, propagation, and decay of $N^*(1535)$, $N^*(1650)$, and $N^*(1710)$ intermediate nucleon resonance states. The coupling constants at the resonances-nucleon-meson vertices were determined from the experimental branching ratios of the decays of the resonances into the relevant channels. Here again we used the same coupling constants as those used in the previous applications of the model at vertices that appeared also in those calculations. The interference terms among various amplitudes are included in the total transition matrix.

To describe the data at the near threshold beam energies, the FSI effects among the outgoing particles are included by a generalized Watson-Migdal method which allows us to have these effects in all three two-body subsystems of the outgoing channel. This method involves a parameter determined from the constraint that in the limit of FSI in only the NN subsystem, the result of the usual Watson method is reproduced.

In this paper, we presented the analysis of the data for total cross sections for the $pp \to pp\eta$ and $pn \to pn\eta$ reactions and for the η angular distributions in the former reaction. With the same set of vertex parameters, the model provides a good description of the data for the $pp \to pp\eta$ reaction at higher as well as near threshold beam energies, except for the excess energies below 15 MeV where our calculations underpredict the experimental data. The experimental total cross sections

of the $pn \to pn\eta$ reaction are also well described by our model. The data for the η angular distributions in the case of $pp \to pp\eta$ reaction are also well reproduced at two beam energies. Imprecise knowledge of the ηN scattering amplitudes and noninclusion of the three-body effects are the most likely reasons for underestimation of the pp channel data by our model at very low beam energies.

In this study, we have not investigated the observables related to meson energy dependence, e.g., final pp and ηp invariant mass distributions. There are some open theoretical issues concerning the explanation of the corresponding experimental data. While in Ref. [30], the inclusion of contributions of the non-s-wave states in the pp subsystem were found to be essential to explain these data, the three-body effects in the $pp\eta$ system and not the contribution of the higher partial waves were shown to be crucial for this purpose by the authors of Ref. [32]. At this stage, our theory excludes both these effects. Extension of our model to include these mechanisms is vital before we can make some meaningful contribution toward settling of this issue.

Within our model, one-pion exchange processes make the largest contributions to cross sections in the entire energy regime. Despite our using a large coupling constant for the $N^*(1535)N\rho$ vertex, the cross sections of the ρ-meson exchange process are still lower than those of the pion exchange mechanism. Therefore, ρ-meson exchange being the dominant mechanism of $N^*(1535)$ resonance excitation [28] is not supported by our calculations. The individual contributions of the ω-meson exchange diagrams are very small everywhere. On the other hand, the σ exchange terms make relatively larger contributions.

The excitation of the $N^*(1535)$ resonance dominates the $NN\eta$ production at both higher and near threshold beam energies. The contributions of $N^*(1650)$ and $N^*(1710)$ are small in comparison. However, the interference among various resonance contributions is not negligible. Unlike the $NN\pi$ vertex, where there is a clear preference for the PV coupling, the present reaction does not distinguish between PS and PV couplings at the $N^*N\eta$ vertex involving spin-1/2 even or odd parity resonances. We point out that the mechanism of the $pp\eta$ production via preferential excitation of the $N^*(1535)$ intermediate baryonic resonance state in the one-pion exchange process has received support recently from an experimental study [82] of the analyzing powers of the $\bar{p} + p \to p + p + \eta$ reaction.

This work fixes the parameters of the effective Lagrangian model for most of the vertices involved in the η-meson production processes. An interesting further check of this model will be provided by the analysis of the η photoproduction data on nucleons (see, e.g., Refs. [83,84]). An exciting recent result is that the integrated cross section of the photoproduction of η meson on neutrons shows an additional maximum at center-of-mass energies around 1.66 GeV. This has recently been explained in terms of the excitation of the $N^*(1650)$ and $N^*(1650)$ resonance states [85]. Furthermore, the vertex parameters derived by us will also be useful in applications of the effective Lagrangian method in describing the production of η-mesic nuclei in proton and photon induced reactions (see, e.g., Refs. [86,87]).

ACKNOWLEDGMENTS

The author is thankful to Andrzej Deloff for several useful correspondence regarding the off-shell pp FSI method presented in Ref. [61] and for his help in implementing the calculations based on this method. Useful discussions with Horst Lenske, Jerry Miller, Ulrich Mosel, Pawel Moskal, and Madeleine Soyeur are gratefully acknowledged.

APPENDIX: FINAL STATE INTERACTION AMPLITUDES FOR THREE-PARTICLE STATES

We give here some clarifications and steps leading to the derivation of Eq. (23).

The total Hamiltonian of the three-particle system is written as $H = H_0 + U$, where H_0 is the kinetic energy operator of the system and the interaction U is taken as $U = U_{23} + U_{31} + U_{12} \equiv U_1 + U_2 + U_3$ assuming that the three-particle states interact by means of the additive pair interactions represented by U_k. Green's functions corresponding to H and H_0 are, respectively,

$$G^{(\pm)}(E) = \lim_{\epsilon \to 0} \frac{1}{E - H_0 - U \pm i\epsilon}, \tag{A1}$$

$$G_0^{(\pm)}(E) = \lim_{\epsilon \to 0} \frac{1}{E - H_0 \pm i\epsilon}. \tag{A2}$$

We will also need the Hamiltonian describing the two particles interacting while the third one is free, namely, $H_k = H_0 + U_k$ and the corresponding Green's functions

$$G_k^{(\pm)}(E) = \lim_{\epsilon \to 0} \frac{1}{E - H_0 - U_k \pm i\epsilon}. \tag{A3}$$

The full three-body transition operator T satisfies the Lipmann-Schwinger equations

$$T(E) = U + UG_0T(E), \tag{A4}$$

which can also be written as

$$T(E) = \sum_k U_k + \sum_k U_k G_0 T(E). \tag{A5}$$

Equation (A5) leads to the iteration

$$\begin{aligned} T(E) = {} & \sum_k [U_k + U_k G_0 U_k + U_k G_0 U_k G_0 U_k + \cdots] \\ & + \sum_{k \neq j} [U_k + U_k G_0 U_k + \cdots] G_0 \\ & \times [U_j + U_j G_0 U_j + \cdots] + \cdots. \end{aligned} \tag{A6}$$

In the study of the final state interaction problems, one usually has in addition to potential U [which is responsible for the transition from the initial state to the free final states characterized by the transition matrix T_0 in Eq. (22)], an additional interaction V that describes a type of internal interaction among the constituents of the final state. The total Hamiltonian is then written as $H_0 + U + V$, and one can make use of the standard two-potential formalism of Goldberger and Watson (see, e.g., Ref. [42]) to write the total scattering matrix

element (T_{fi}) as a sum of two terms, one of them involving the matrix elements of the interaction U between the exact initial state wave function and the final scattering state wave function corresponding to interaction V. From the general theory, we can write

$$T_{fi} = \langle \chi_f | U + V | \psi_i^{(+)} \rangle, \tag{A7}$$

where $\psi_i^{(+)}$ completely describes the initial state with the outgoing wave boundary condition, and χ_f is the final plane wave state. One can eliminate χ_f by introducing wave functions $\phi_f^{(-)}$, which are the eigenfunctions of the Hamiltonian $H_0 + V$, as

$$\phi_f^{(-)} = \chi_f + G_0^{(-)} V \phi_f^{(-)}. \tag{A8}$$

Substituting Eq. (A8) into Eq. (A7), one gets after some manipulation,

$$T_{fi} = \langle \phi_f^{(-)} | U | \psi_i^{(+)} \rangle + \langle \phi_f^{(-)} | V | \chi_i \rangle, \tag{A9}$$

where χ_i is the initial plane wave state. The final state interactions of interest are contained in $\phi_f^{(-)}$.

In applications of relevance to us, the second term of Eq. (A9) would vanish, because we assume V cannot create real mesons. Equation (23) can be obtained by using an iteration similar to that given by Eq. (A6) in the remaining (first) term of Eq. (A9). The amplitude T_0 is defined in the same way as the first term of Eq. (A9) with a plane wave final state. The amplitude T_k in the second term of Eq. (23) represents the matrix elements of the interaction V_k between the plane wave and the scattering states of particle ij. We define V_k for the partition k in the same way as U_k.

[1] K. G. Wilson, Phys. Rev. D **10**, 2445 (1974).
[2] D. B. Leinweber, W. Melnitchouk, D. G. Richards, A. G. Williams, and L. M. Zanotti, in *Lattice Hadron Physics,* edited by A. Kalloniatis, D. Leinweber, A. Williams (Springer, Berlin, 2005), p. 71; J. M. Zanotti, B. Lasscock, D. B. Leinweber, and A. G. Williams, Phys. Rev. D **71**, 034510 (2005); R. D. Young, D. B. Leinweber, and A. W. Thomas, *ibid.* **71**, 014001 (2005).
[3] P. Mosal, M. Wolke, A. Khoukaz, and W. Oelert, Prog. Part. Nucl. Phys. **49**, 1 (2002).
[4] H. O. Meyer *et al.*, Phys. Rev. C **63**, 064002 (2001), and references therein.
[5] J. Balewski *et al.*, Phys. Lett. **B420**, 211 (1998).
[6] S. Sewerin *et al.*, Phys. Rev. Lett. **83**, 682 (1999).
[7] P. Kowina *et al.*, Eur. Phys. J. A **22**, 293 (2004).
[8] M. Abdel-Bary *et al.*, Phys. Lett. **B595**, 127 (2004).
[9] A. Abd El-Samad *et al.*, Phys. Lett. **B632**, 27 (2006).
[10] H. Calen *et al.*, Phys. Rev. C **58**, 2667 (1998).
[11] H. Calen *et al.*, Phys. Lett. **B458**, 190 (1999).
[12] J. Smyrski *et al.*, Phys. Lett. **B474**, 182 (2000); F. Hibou *et al.*, *ibid.* **B438**, 41 (1998); H. Calen *et al.*, *ibid.* **B366**, 39 (1996); E. Chiavassa *et al.*, *ibid.* **B322**, 270 (1993); A. M. Bergdolt *et al.*, Phys. Rev. D **48**, R2969 (1993).
[13] M. Abdel-Bary *et al.*, Eur. Phys. J. A **16**, 127 (2003).
[14] F. Balestra *et al.*, Phys. Rev. C **69**, 064003 (2004).
[15] P. Moskal *et al.*, Phys. Rev. C **69**, 025203 (2004).
[16] C. Dover and P. Fishbane, Phys. Rev. Lett. **64**, 3115 (1990).
[17] See, e.g., Z. Papandreou, AIP Conf. Proc. **814**, 453 (2005).
[18] N. Mathur, Y. Chen, S. J. Dong, T. Draper, I. Horvath, F. X. Lee, K. F. Liu, and J. B. Zhang, Phys. Lett. **B605**, 137 (2005); C. Hanhart, Acta Phys. Slov. **56**, 193 (2005).
[19] H. C. Chiang, E. Oset, and L. C. Liu, Phys. Rev. C **44**, 738 (1991).
[20] A. Fix and H. Arenhövel, Phys. Rev. C **66**, 024002 (2002).
[21] Q. Haider and L. C. Liu, Phys. Rev. C **66**, 045208 (2002).
[22] M. Pfeiffer *et al.*, Phys. Rev. Lett. **92**, 252001 (2004).
[23] A. Sibirtsev, J. Haidenbauer, J. A. Niskanen, and Ulf-G. Meissner, Phys. Rev. C **70**, 047001 (2004).
[24] International Workshop on η-nucleus Physics, May 8–12, 2006, Jülich, Germany, summary is available at arXiv:nucl-th/0610011.
[25] W. Cassing, V. Metag, U. Mosel, and K. Niita, Phys. Rep. **188**, 363 (1988).
[26] T. Vetter, A. Engel, T. Biro, and U. Mosel, Phys. Lett. **B263**, 153 (1991).
[27] A. Moalem, E. Gedalin, L. Razdolskaja, and Z. Shorer, Nucl. Phys. **A600**, 445 (1996); E. Gedalin, A. Moalem, L. Razdolskaya, *ibid.* **A634**, 368 (1998); **A650**, 471 (1999).
[28] G. Fäldt and C. Wilkin, Phys. Scr. **64**, 427 (2001).
[29] K. Nakayama, J. Speth, and T. -S. H. Lee, Phys. Rev. C **65**, 045210 (2002).
[30] K. Nakayama, J. Haidenbauer, C. Hanhart, and J. Speth, Phys. Rev. C **68**, 045201 (2003).
[31] V. Baru, H. Haidenbauer, C. Hanhart, Y. Kalashnikova, and A. Kudryavtsev, Phys. Lett. **B586**, 53 (2004).
[32] A. Fix and H. Arenhövel, Phys. Rev. C **69**, 014001 (2004).
[33] A. Engel, R. Shyam, U. Mosel, and A. K. Dutt-Majumder, Nucl. Phys. **603**, 387 (1996).
[34] R. Shyam and U. Mosel, Phys. Lett. **B425**, 1 (1998).
[35] R. Shyam, Phys. Rev. C **60**, 055213 (1999); R. Shyam, G. Penner, and U. Mosel, *ibid.* **63**, 022202(R) (2001); R. Shyam, *ibid.* **73**, 035211 (2006).
[36] R. Shyam and U. Mosel, Phys. Rev. C **67**, 065202 (2003).
[37] M. Schäfer, H. C. Dönges, A. Engel, and U. Mosel, Nucl. Phys. **A575**, 429 (1994).
[38] S. Weinberg, Phys. Rev. **166**, 1568 (1968).
[39] V. Bernard, N. Kaiser, and Ulf-G. Meissner, Int. J. Mod. Phys. E **4**, 193 (1995).
[40] C. Hanhart, Phys. Rep. **397**, 155 (2004).
[41] R. Machleidt, K. Hollinde, and Ch. Elster, Phys. Rep. **149**, 1 (1987).
[42] M. L. Goldberger and K. M. Watson, *Collision Theory* (Wiley, New York, 1969), pp 549.
[43] J. Gillespie, in *Final-State Interaction*, Adv. Phys. Monographs, edited by K. M. Watson (Holden-Day, San Francisco, 1964), and references therein.
[44] A. Deloff, talk given at COSY-11 Meeting, Cracow, June 1–3, 2004 (unpublished), arXiv:nucl-th/0406069.
[45] T. Ericson and W. Weise, *Pions and Nuclei* (Clarendon, Oxford, 1988).
[46] G. Penner and U. Mosel, Phys. Rev. C **66**, 055211 (2002); **66**, 055212 (2002); G. Penner, Ph.D. thesis, Universität Giessen, 2002, available (in English) at the URL http://theorie.physik.uni-giessen.de

[47] J. D. Bjorken and S. D. Drell, *Relativistic Quantum Mechanics* (McGraw-Hill, New York, 1964).
[48] M. Benmerrouche, N. C. Mukhopadhyay, and J. F. Zhang, Phys. Rev. D **51**, 3237 (1995).
[49] W. Grein and P. Kroll, Nucl. Phys. **A338**, 332 (1980).
[50] C. Bennhold, Nucl. Phys. **A585**, 313c (1995).
[51] M. Kirchbach and L. Tiator, Nucl. Phys. **A605**, 385 (1996).
[52] W. M. Yao *et al*. (Particle Data Group), J. Phys. G: Nucl. Part. Phys. **33**, 1 (2006).
[53] T. Feuster and U. Mosel, Nucl. Phys. **A612**, 375 (1997).
[54] T. Feuster and U. Mosel, Phys. Rev. C **58**, 457 (1998).
[55] R. Shyam, H. Lenske, and U. Mosel, Nucl. Phys. **A764**, 313 (2006).
[56] J. J. Sakurai, *Currents and Mesons* (University of Chicago, Chicago, 1969); Ann. Phys. (NY) **11**, 1 (1960).
[57] J. Dubach, W. M. Kloet, and R. R. Silbar, Phys. Rev. C **33**, 373 (1986).
[58] V. Bernard, N. Kaiser, and Ulf-G. Meissner, Eur. Phys. J. A **4**, 259 (1999).
[59] A. Moalem, E. Gedalin, L. Razdolskaja, and Z. Shorer, Nucl. Phys. **A600**, 455 (1996).
[60] B. L. Druzhinin, A. E. Kudryavtsev, and V. E. Tarasev, Z. Phys. A **359**, 205 (1997).
[61] A. Deloff, Phys. Rev. C **69**, 035206 (2004).
[62] A. Sibirtsev, J. Haidenbauer, H.-W. Hammer, and U.-G. Meissner, Eur. Phys. J. A **29**, 363 (2006).
[63] A. I. Titov, B. Kämpfer, and B. L. Reznik, Eur. Phys. J. A **7**, 543 (2000).
[64] M. Soyeur and M. F. M. Lutz, Int. J. Mod. Phys. **A22**, 333 (2007).
[65] A. M. Green and S. Wycech, Phys. Rev. C **71**, 014001 (2005).
[66] M. F. M. Lutz, Gy. Wolf, and B. Friman, Nucl. Phys. **A706**, 431 (2002).
[67] E. Gedalin, A. Moalem, and L. Razdolskaya, Nucl. Phys. **A634**, 368 (1998); **A650**, 471 (1999).
[68] H. Garcilazo and M. T. Pena, Phys. Rev. C **66**, 034606 (2002).
[69] A. M. Gasparyan, J. Haidenbauer, C. Hanhart, and J. Speth, Phys. Rev. C **68**, 045207 (2003).
[70] H. P. Noyes, Annu. Rev. Nucl. Sci. **22**, 465 (1972).
[71] C. Hanhart and K. Nakayama, Phys. Lett. **B454**, 176 (1999).
[72] V. Baru, A. M. Gasparyan, J, Haidenbauer, A. E. Kudryavtsev, and J. Speth, Phys. At. Nucl. **64**, 579 (2001) [Yad. Fiz. **64**, 633 (2001)].
[73] A. Gasparyan, J. Haidenbauer, and C. Hanhart, Phys. Rev. C **72**, 034006 (2005).
[74] *Landolt-Börnstein: Numerical Data and Functional Relationships in Science and Technology, New Series*, edited by H. Schopper (Springer, Berlin, 1988), I/12.
[75] B. Lopez Alvaredo and E. Oset, Phys. Lett. **B324**, 125 (1994).
[76] W.-T. Chiang, S. N. Yang, L. Tiator, and D. Drechsel, Nucl. Phys. **A700**, 429 (2002).
[77] A. B. Santra and B. K. Jain, Nucl. Phys. **A634**, 309 (1998).
[78] M. Post, S. Leupold, and U. Mosel, Nucl. Phys. **A689**, 753 (2001).
[79] D. O. Riska and G. E. Brown, Nucl. Phys. **A679**, 577 (2001).
[80] T. S. H. Lee and D. O. Riska, Phys. Rev. Lett. **70**, 2237 (1993).
[81] C. J. Horowitz, H. O. Meyer, and D. K. Griegel, Phys. Rev. C **49**, 1337 (1994).
[82] R. Czyzykiewicz *et al*., Phys. Rev. Lett. **98**, 122003 (2007).
[83] V. Kuznetsov *et al*., in *NSTAR 2005: Proceedings of the Workshop on the Physics of Excited Nucleons,* edited by S. Capstick, V. Crede, and P. M. Eugenio (World Scientific, Singapore, 2006).
[84] B. Krusche *et al*., Talk given at International Workshop on η Nucleus Physics, May 8–12, 2006, Jülich, Germany, arXiv:nucl-th/0610011 (unpublished)
[85] V. Shklyar, H. Lenske, and U. Mosel, arXiv:nucl-th/0611036 (unpublished).
[86] M. Kh. Anikina *et al*., arXiv:nucl-ex/0412036 (unpublished).
[87] V. A. Baskov, J. P. Bocquet, V. Kouznetsov, A. Lleres, A. I. L'vov, L. N. Pavlyuchenko, V. V. Polyanski, D. Rebrevend, G. A. Sokol, arXiv:nucl-ex/0306011 (unpublished).